KSME

Springer

Journal of Mechanical Science and Technology 37 (4) 2023

Original Article
DOI 10.1007/s12206-023-0317-9

Keywords:
· LWR primary system
· Stainless steel
· Stress corrosion cracking
· Compressive residual stress
· Surface crack nondamaging technology
· Reliability improvement of maintenance

Correspondence to:
Ki-Woo Nam
namkw@pknu.ac.kr

Citation:
Gu, K.-H., Ando, K., Nam, K.-W. (2023). Analytical study on rationalize and reliability improvement of maintenance against stress corrosion cracking in stainless steel welds of LWR primary system. Journal of Mechanical Science and Technology 37 (4) (2023) 1773~1780. http://doi.org/10.1007/s12206-023-0317-9

Received January 8th, 2022
Revised December 14th, 2022
Accepted January 10th, 2023

† Recommended by Editor Chongdu Cho

Analytical study on rationalize and reliability improvement of maintenance against stress corrosion cracking in stainless steel welds of LWR primary system

Kyoung-Hee Gu[1], Kotoji Ando[2] and Ki-Woo Nam[1,3]

[1]Dept. of Marine Design Convergence Engineering, Pukyong National University, Busan, Korea, [2]Faculty of Engineering, Yokohama Nat'l Univ., Yokohama, Japan, [3]Dept. of Materials Science and Engineering, Pukyong National University, Busan, Korea

Abstract SCC (stress corrosion cracking) may occur in stainless steel welds of the LWR primary systems, which required the welding repair after detecting it over nondestructive inspection (NDI) during the regular inspections. Recently, a new peening method was developed to convert the tensile residual stress of the weld into compressive residual stress, which relieved the SCC issue in the new plant although SCC problems still exist in conventional plant. It was found that fatigue crack and SCC can be rendered harmless by the compressive residual stress over a peening method. This paper proposes a method for increasing the validity and reliability of the weld maintenance for SCC by the following methods. ① Evaluate the depth (a_{hml}) of SCC cracks that can be rendered harmless by peening in advance. ② Detect the cracks of approximately 0.7 a_{hml} or more by NDI. ③ Repair only crack of 0.7 a_{hml} or more by welding. ④ Apply peening to all welds. This paper proposes a method for evaluating a_{hml}, and analyzed the dependence of residual stress and crack aspect ratio (As) via peening. The study showed that it was possible to improve the reliability and rationalize the maintenance for SCC by applying the surface crack nondamaging technology.

1. Introduction

Stress corrosion cracking (SCC) may occur often in welded parts of stainless steel, which are used in chemical plants and primary systems of light water reactors. The problem of corrosion prevention is being studied in various ways (peening, coating, etc.). Koten and Kamaci [1] has been evaluated the corrosion resistance of coated AZ31B with stearic acid and magnesium nitart-containing coating materials. The tensile residual stress in new plants are converted into the compressive residual stress by peening the weld part to prevent SCC [2]. The conventional plant has adopted three methods of SCC countermeasure. After detecting as many SCC as possible by NDI, ① Defects are evaluated according to ASME standards, etc. [3, 4], initially. Then only unacceptable defects are repaired by welding. ② After that, all defects are repaired by welding. ③ All defects are peened after welding repair.

Method ③ is a very excellent method although it needs some improvements as follows. The reason is that a technology was developed to rendered harmless fatigue crack and SCC surface crack [5-7] by peening. This technology has the following advantages.

1) Assuming that the crack depth that can be rendered harmless by peening is a_{hml}, the detectable crack depth by NDI is approximately 0.8 a_{hml}. This help shortening NDI time and improving reliability. Even if cracks as small as a_{hml} cannot be detected, these cracks can be rendered almost harmless, leading to no safety problem.

2) Since the number of defects detected by NDI is reduced, the number of weld repair por-

tions is reduced.

From the above viewpoints, this paper presents the evaluation method of the harmless crack depth (a_{hml}) of SCC, and investigated the effect of the compressed residual stress distribution by peening and the crack aspect ratio (As) on a_{hml} . Next, the high reliability of SCC maintenance and the shortening of maintenance time can be achieved by comparing the crack depth (a_{NDI}), detected by NDI with a_{hml} (a_{hml} > a_{NDI} by introducing a large and deep compressive residual stress).

In order to apply this method to conventional plants, the following five steps are required.

I) Evaluate the harmless crack depth (a_{hml}) according to the applied peening method.

II) Apply NDI that can reliably detect cracks with a crack depth of approximately 0.8 a_{hml} .

III) Detect cracks with a depth of 0.8 a_{hml} or more by NDI certainly.

IV) All the above crack are repaired by welding.

V) Peening is applied to all welds to convert tensile residual stress into compressive residual stress.

Therefore, in this study, it was found that the LWR primary system stainless steel welds can ensure reliability and rationality for SCC maintenance with an application of surface crack nondamaging technology by peening.

2. Materials, properties, design stress, and residual stress distribution

The specimen for the analysis was a plate with a width (2*w*) and thickness (*t*) of 400 and 20 mm, respectively, and constituted a stainless steel weld portion. The material properties [8] of interest were the tensile strength (σ_u), the yield stress (σ_y) and Vickers hardness of 590 MPa, 310 MPa and 193, respectively. $K_{sc(l)}$ for large cracks is 4.5, 6.6, and 8.2 MPa $\sqrt{m}$. Fig. 1 shows a schematic of the model. The four different values of *As* (*As* = *a/c*) were 1.0, 0.6, 0.3, and 0.1. It was also assumed that there was no bead at the weld toe. The design tensile stress (σ_{DE}) (opening mode) was 100 MPa, which was equal to the allowable stress; however because the design tensile stress often differs depending on the position of the components, the 60, 80, and 120 MPa were also analyzed.

The welded joint was assumed to be a butt joint with an X-groove without excess weld metal, and the groove depths on the front and back surfaces were freely selected in consideration of workability. The peening portion was determined to satisfy the following conditions A) and B). A) The part where the sum of the tensile weld residual stress and design stress exceeds the yield stress (σ_y). The reason is that work hardening due to yielding induces the initiation of SCC crack. B) The part where grain boundaries are sensitized by welding heating. This part needs to be determined in consideration of the welding heat input and the temperature between welding pass.

Fig. 2 shows three types of compressive residual stress distributions by peening, named RS1, RS2, and RS3. Table 1 shows the compressive residual stress (σ_0) at the surface, maximum compression residual stress (σ_m), and crossing point (d_0), at which the compressive residual stress becomes zero. σ_0 was set with reference to the residual stress distribution via laser peening [8]. As a result, three types of residual stress distributions were assumed.

Table 1. Compressive residual stress by peening.

	σ_0 (MPa)	σ_m (MPa)	d_0 (mm)
RS1	–160	–180	0.8
RS2	–130	–160	0.6
RS3	–100	–140	0.4

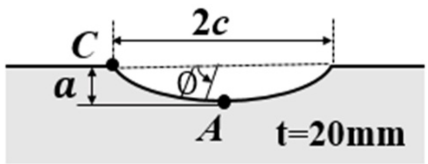

Fig. 1. Schematic illustration of a semi-elliptical crack in a finite plate.

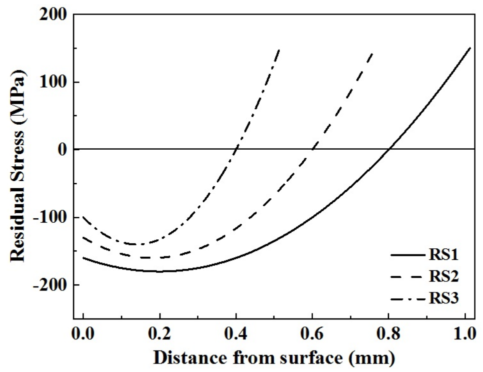

Fig. 2. Three types of compressive residual stress distribution by peening (RS1, RS2, and RS3).

3. Analysis method and detection probability of crack

3.1 Evaluation of threshold stress intensity factor of small SCC propagation ($K_{sc(s)}$)

$K_{sc(l)}$ does not depend on the crack size, as the small-scale yield condition is satisfied for large cracks as well. However, as it is not satisfied for small cracks, the threshold stress intensity factor of SCC propagation (K_{sc}) is a value that depends on the crack size. Using a method such as Milne et al. [9], the author et al. was proposed Eq. (1) [10], which describes the relationship between $K_{sc(l)}$ and K_{sc} for a crack length of 2*l* in an infinite plate, and a tensile stress σ_{sc} .

$$l\left\{\sec\frac{\pi\sigma_{sc}}{2\sigma_y}-1\right\}=\frac{\pi}{8}\left(\frac{K_{sc(l)}}{\sigma_y}\right)^2 . \tag{1}$$

Each variable on the right-hand side of Eq. (1) has a characteristic value. The crack length dependence of K_{sc} in a small crack can be obtained using Eq. (2).

$$K_{sc} = \sigma_{sc}\sqrt{\pi l}\ . \tag{2}$$

Thus, K_{sc} increases with the crack length, with its saturation value being $K_{sc(l)}$. Eq. (3) was obtained by eliminating σ_{sc} from Eqs. (1) and (2).

$$K_{sc} = 2\sigma_y\sqrt{\frac{l}{\pi}}\cos^{-1}\left[\left\{\frac{\pi}{8l}\left(\frac{K_{sc(l)}}{\sigma_y}\right)^2+1\right\}^{-1}\right]. \tag{3}$$

When Eqs. (2) and (3) are applied to a semi-elliptical crack in a finite plate, the equivalent half-crack length (l_e) given by Eq. (4), and is substituted for *l* in Eqs. (2) and (3).

$$\sqrt{\pi l_e} = \alpha\sqrt{\pi a} \tag{4}$$

where α is the shape correction factor for the semi-elliptical crack in the finite plate. Eq. (5) is given by the Newman-Raju equation [11] as follows:

$$K = \frac{F\left(\frac{a}{t},\frac{a}{c},\frac{c}{w},\phi\right)}{\sqrt{Q\left(\frac{a}{c}\right)}}\sigma_T\sqrt{\pi a} = \alpha\sigma_T\sqrt{\pi a} \tag{5}$$

where *F* and *Q* are the shape correction factors; *t* is the thickness of the finite plate; *w* is the half-width of the finite plate; and *ϕ* is the angle of the semi-elliptical crack. α_A and α_C are given at ϕ = 90 and 0°, respectively, as shown in Fig. 1.

3.2 Evaluation of a_{hml}

a_{hml} is given by Eq. (6) from the sum of K_{app} from the design stress (σ_{DE}) and K^{Pr} from the residual stress via peening.

$$K_{app}^{Pr} = K_{app} + K^{Pr} = K_{SC(S)} \tag{6}$$

where K_{app} is the stress intensity factor obtained from Eq. (5) using σ_{DE} . K^{Pr} due to the residual stress distribution of Fig. 2 is obtained by the fourth-order polynomial in Eq. (7) from API-RP579 [12].

$$K^{Pr} = [G_0\sigma_0 + G_1\sigma_1\left(\frac{a}{t}\right) + G_2\sigma_2\left(\frac{a}{t}\right)^2 + G_3\sigma_3\left(\frac{a}{t}\right)^3 + G_4\sigma_4\left(\frac{a}{t}\right)^4)]\sqrt{\frac{\pi a}{Q}}f_w \tag{7}$$

$$\mathrm{Q} = 1.0 + 1.464\left(\frac{a}{c}\right)^{1.65},\quad f_w = \left\{\sec\left(\frac{\pi c}{2w}\sqrt{\frac{a}{t}}\right)\right\}^{0.5}$$

where $G_0 - G_4$ are the shape correction coefficients of the K^{Pr} , ***a*** and ***c*** indicate the depth and length of the semicircular crack, respectively; *t* is the thickness of the plate; and $\sigma_1 - \sigma_4$ are coefficients obtained from the fourth-order polynomial in Eq. (8).

$$\sigma(x) = \sigma_0 + \sigma_1\left(\frac{x}{t}\right) + \sigma_2\left(\frac{x}{t}\right)^2 + \sigma_3\left(\frac{x}{t}\right)^3 + \sigma_4\left(\frac{x}{t}\right)^4 \tag{8}$$

where x is the distance in the depth direction from the surface on which the crack is present. The crack depth dependence of K_{SC} is obtained from Eqs. (1)-(5).

3.3 Detection probability of a fatigue crack using NDI

Rummel et al. [13] conducted detailed studies on the detection probability of semi-elliptical fatigue cracks, and reported that ultrasonic detection method showed the highest probability of fatigue crack detection. Cracks with 100 % detection probability obtained under optimal conditions in the laboratory using this method had 2*c* and *a* of 12 and 4 mm [14], respectively. In addition, the minimum crack size obtained under optimum conditions in the laboratory was 0.17 mm along both depth and length directions by ultrasonic detection method [13]. However, this study was published in 1974. With recent technological advancements, SCC with a depth of 0.4 mm can be measured [15]. However, because their study did not report the crack length, the crack was assumed to be a semi-elliptical crack.

Nevertheless, the ultrasonic detection method is a high-performance crack detection method; here, two NDIs (1) and (2) were assumed. In NDI(1), it was assumed that a semi-elliptical crack with 2*c* and *a* of 0.6 and 0.3 mm, respectively, had sufficient crack detection probability. The area and depth of this crack area were defined as $S_{NDI(1)}$ and $a_{NDI(1)}$, respectively. However, this SCC crack is known to require a long time to detect with sufficient probability.

In contrast, a crack with 60 % detection probability in the study by Rummel et al. [13] had 2*c* and *a* of 1.4 and = 0.25 mm [14], respectively. In NDI(2), it was assumed that the semi-elliptical SCC had a sufficient crack detection probability. The area and depth of this crack were defined as $S_{NDI(2)}$ and $a_{NDI(2)}$, respectively. Considering the measurement of the reflection echo from a crack using the ultrasonic detection method, the echo intensity would depend on the crack area. The area (*S*) of the semi-elliptical crack can be obtained using Eq. (9).

$$S = \pi ac / 2\ . \tag{9}$$

Thus, for the same *S* value of a semi-elliptical crack, even if *As* changes the detection probability of the crack would be the same. The relationship between a_{NDI} and *As* was evaluated using Eq. (10).

$$S_{NDI} = \pi a_{NDI}{}^2 / 2A_S \ . \tag{10}$$

4. Results and discussion

4.1 Evaluation of a_{hml} via peening

4.1.1 Dependence of a_{hml} on as at σ_{DE} = 100 MPa

Fig. 3 shows the dependence of a_{hml} by peening at *As* = 1.0. Figs. 3(a) and (b) show the results at points *A* and *C*, respectively. The maximum crack depth that could be rendered harmless by peening was evaluated using Eq. (6). For all residual stresses, the effect of $K_{sc(l)}$ on a_{hml} was significantly small because K_{app}^{Pr} increased sharply before crossing the line of $K_{sc(l)}$ = 4.5 $\text{MPa}\sqrt{m}$. Moreover, as all a_{hml} values were larger than approximately 0.5 mm, the difference was small regardless of whether a_{hml} was evaluated by K_{sc} or $K_{sc(l)}$. The same tendency is observed in Figs. 4 and 5. This analysis was different from the fatigue fracture of high-strength steel [6], and it can be said that the small-crack problem was not particularly important.

a_{hml} evaluated from Fig. 3 differed between points *A* and *C*; that is, point *A* had a much smaller than point *C*. For example, in the case of $K_{sc(l)} = 8.2\,\text{MP}\sqrt{\text{m}}$, a_{hml} of RS1 was approximately 1.14 and 2.86 mm at points *A* and *C*, respectively. The smaller crack size was defined as a_{hml} . Thus, a_{hml} was determined at point *A* for all values of *As*.

Fig. 4 shows only the results of a_{hml} at point *A* for *As* = 0.6, 0.3, and 0.1. a_{hml} was determined at point *A* for all values of *As* because σ_0 compressive residual stress was always applied at point *C*, and the absolute values except RS3 were larger than the tensile stress value of the design, whereas at point *A*, the tensile residual stress by peening and welding rapidly increased after d_0 .

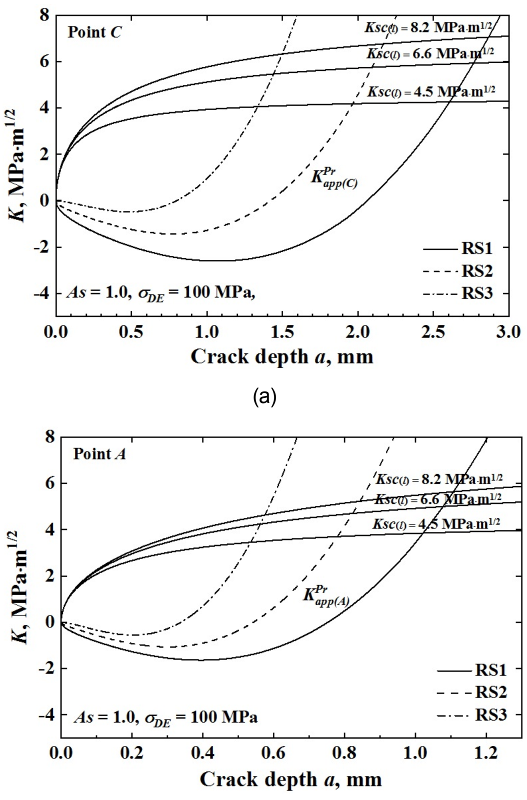

Fig. 3. a_{hml} by peening for *As* = 1.0: (a) point *A*; (b) point *C*.

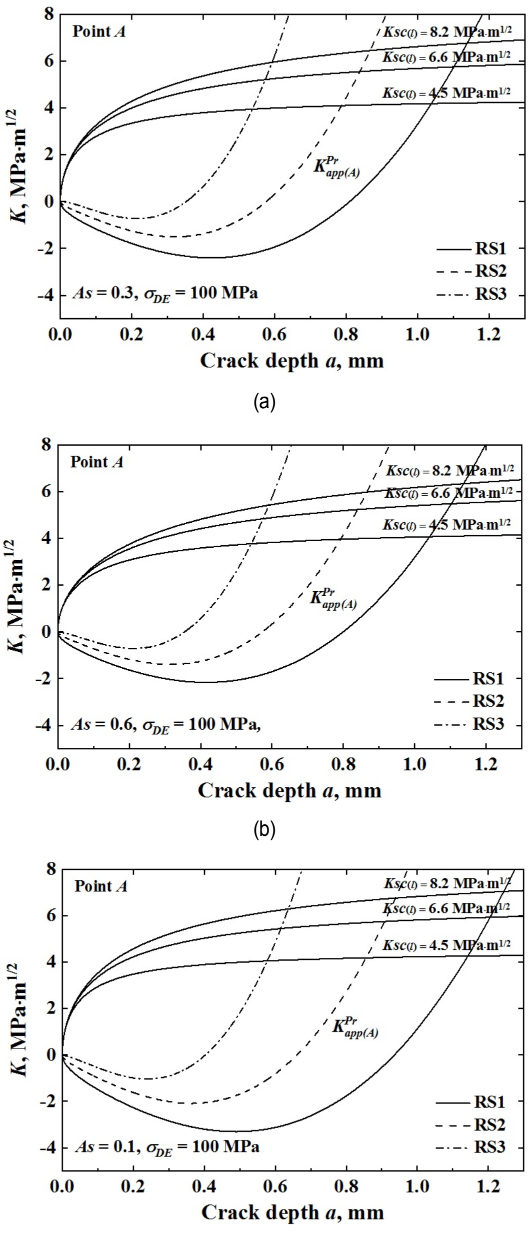

Fig. 4. Evaluation of a_{hml} by peening: (a) *As* = 0.6; (b) *As* = 0.3; (c) *As* = 0.1.

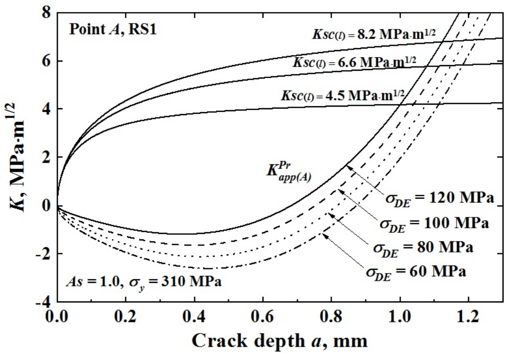

Fig. 5. Variation of a_{hml} with K (σ_{DE} was varied from 60 to 120 MPa for *As* = 1.0 using residual stress RS1).

4.1.2 Dependence of a_{hml} on σ_{DE} for As = 1.0 in RS1

Fig. 5 shows the results of a_{hml} for the case, where the design stress was changed from 60 to 120 MPa when *As* = 1.0, using the residual stress RS1. Fig. 5 also shows the case of σ_y = 310 MPa. The allowable stress was 100 MPa; however, because the stress would often change depending on the location, it was evaluated for allowable stress values of up to 60 MPa. In addition, it was also evaluated for a stress value of 120 MPa, assuming that σ_{DE} should be exceeded.

a_{hml} was determined at point *A* in all the cases. The characteristics are as follows:

1) a_{hml} clearly depended on the σ_{DE}, and it increased at almost equal intervals, as σ_{DE} decreased by 20 MPa.

2) a_{hml} clearly depended on $K_{sc(l)}$, and increased as $K_{sc(l)}$ increases.

4.2 Application of material maintenance of surface SCC-harmless technology via peening

4.2.1 Relevance for SCC maintenance

The dependence of a_{hml} on the residual stress, $K_{sc(l)}$, and *As* at σ_{DE} of 100 MPa is shown in Figs. 3 and 4. Fig. 6 shows the results for $K_{sc(l)}$ = 8.2, 6.6, and 4.5 $\mathrm{MPa}\sqrt{m}$. Figs. 6(a)-(c) show the values of a_{hml} at $K_{sc(l)}$ =8.2, 6.6, and 4.5 $\mathrm{MPa}\sqrt{m}$, respectively. From these figures, it can be seen that the following four characteristics are important for SCC maintenance.

I) It can be seen that a_{hml} did not depend significantly on *As*; however, it exhibited the minimum value for all $K_{sc(l)}$ values, when *As* = 1.0. Therefore, when peening was performed after welding repair, a_{hml} required for maintenance was the value when *As* = 1.0.

II) In consideration of the above, when peening was performed after a welding repair, it was sufficient to detect the cracks exactly with a depth of approximately 80 % of a_{hml} described in ①, followed by repair-welding.

III) a_{NDI} by NDI decreased as *As* decreased, and yielded the lowest value when *As* = 0.1. The residual stress in the direction perpendicular to the weld line was maximum at the outermost surface, and the center of the plate thickness was the compression residual stress when the tensile constraint was not strong. Therefore, the SCC along the weld line was almost always long, and *As* was small. Therefore, if peening is not performed after the NDI and welding repair, it can be said that the crack depth to be detected by NDI would be a shallow crack with *As* = 0.1.

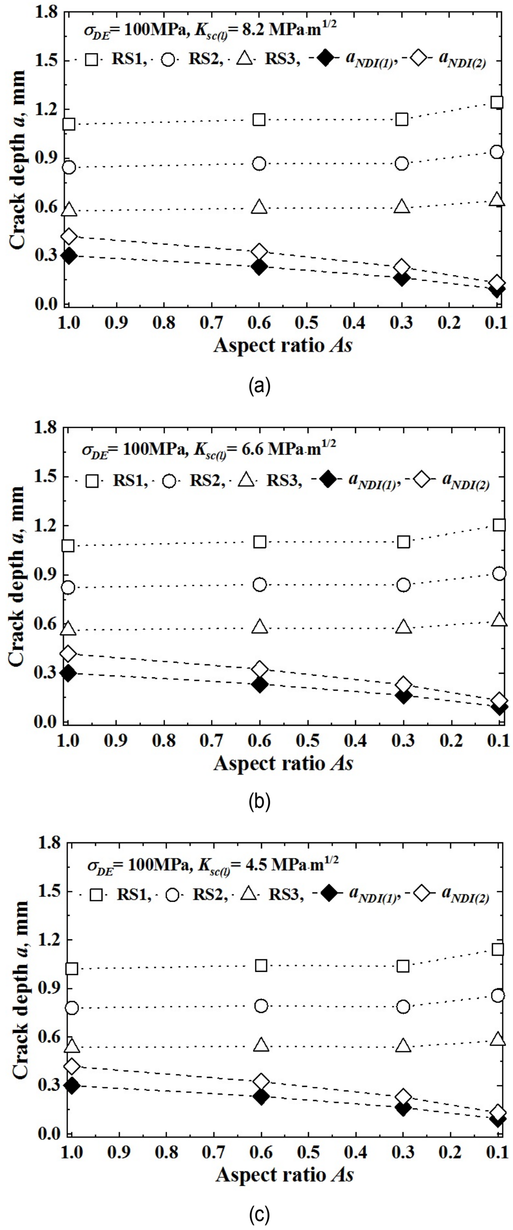

Fig. 6. Variation of a_{hml} with *As* and detectable crack depth ($a_{NDI(1)}$, $a_{NDI(2)}$): (a) $\Delta K_{sc(l)}$ = 8.2 MPa $\sqrt{m}$; (b) $\Delta K_{sc(l)}$ = 6.6 MPa $\sqrt{m}$; (c) $\Delta K_{sc(l)}$ = 4.5 MPa $\sqrt{m}$.

4.2.2 Crack depth and maintenance rationality to be detected by NDI when peening was performed after welding repair

From I) to III), Table 2 are shown the crack depth to be de-

Table 2. a_{hml} and required crack depth detected by NDI as a function of $K_{sc(l)}$ and NDI detectability.

Residual stress by peening	RS1			RS2			RS3		
$K_{sc(l)}$ MPa $\sqrt{m}$	8.2	6.6	4.5	8.2	6.6	4.5	8.2	6.6	4.5
a_{hml} (mm) (As = 1.0)	1.11	1.08	1.02	0.844	0.823	0.780	0.575	0.563	0.535
Required crack depth (mm) detected by NDI	0.89	0.86	0.82	0.68	0.66	0.62	0.46	0.45	0.43
$a_{NDI(1)}$ (mm)	0.32								
$a_{NDI(2)}$ (mm)	0.42								

tected by NDI and repaired by welding. In the case of RS1, the crack depth that must be reliably detected by NDI was 0.82 to 0.89 mm; however, it depended on $K_{sc(l)}$. This value was sufficiently larger than the maximum value of $a_{NDI(1)}$ when *As* = 1.0, which was approximately 0.32 mm. Therefore, as the number of cracks that must be detected was reduced, there was an advantage that the NDI and the welding repair location could be reduced. However, this would not reduce the rationality of maintenance. In contrast, in the case of RS3, the maximum values of a_{hml} and $a_{NDI(1)}$ were similar. Even if an NDI could not detect a crack, the crack could be rendered harmless. Therefore, it can be said that the reliability of maintenance was improved; however, it would not contribute to the rationalization of maintenance. This tendency was almost the same as the case of rationalization of maintenance and improvement of reliability of high-strength steel designed against fatigue limit using surface-crack-harmless technology [16].

4.2.3 No peening after welding repair

In this case, it is necessary to detect even shallow cracks with *As* = 0.1 and repair by welding. The crack depth detectable by NDI was 0.1 to 0.13 mm. These dimensions of the crack must have been detected and repaired by welding. Therefore, the NDI time increased and the number of welding repair points increased. In addition, if these crack dimensions could not be detected, the reliability of maintenance would decrease.

From the above considerations (4.2.1) to (4.2.3), it can be inferred that if a large and deep residual stress is created by peening after welding repair for SCC countermeasures for stainless steel welds, it can contribute to the rationalization of maintenance and improvement of reliability.

4.2.4 Dependence of a_{hml} on σ_{DE}

Fig. 7 shows the dependence of a_{hml} on σ_{DE} (60-120 MPa) for $K_{sc(l)}$ = 8.2, 6.6, and 4.5 $\text{MPa}\sqrt{m}$ and *As* = 1.0. a_{hml} increased almost linearly as σ_{DE} decreased; furthermore, the larger the $K_{sc(l)}$, the larger the a_{hml}. When σ_{DE} was 60 and 100 MPa, the dependence of a_{hml} on *As* was evaluated for all values of $K_{sc(l)}$. The range of a_{hml} is shown by the variation width (I). In all the cases, the minimum and maximum values of a_{hml} were obtained when *As* = 1.0 and 0.1, respectively. Thus,

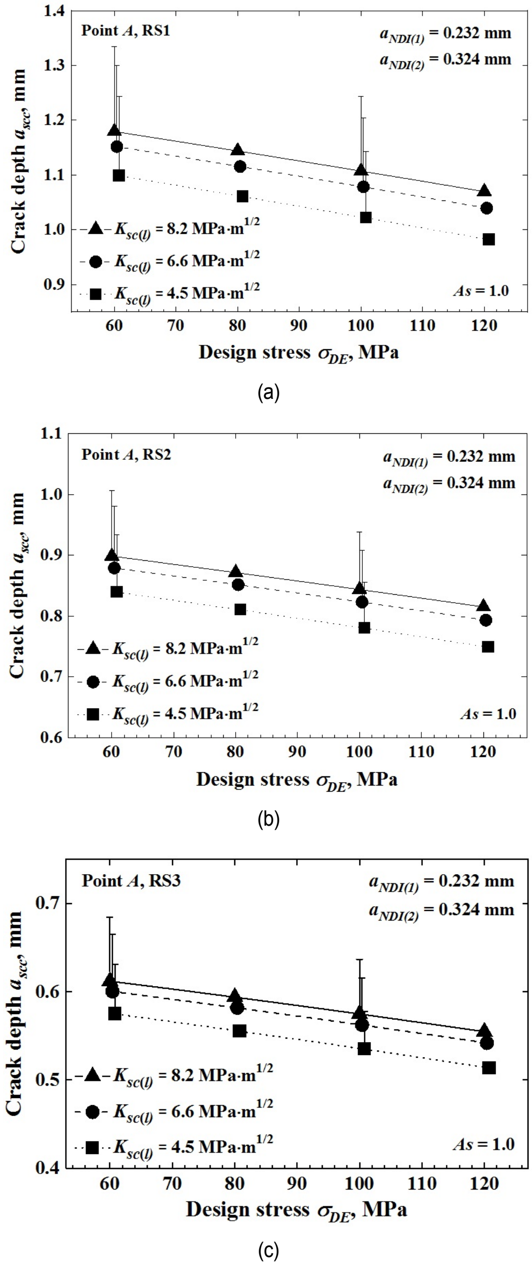

Fig. 7. Variation of crack depth on σ_{DE}: (a) RS1; (b) RS2; (c) RS3.

when σ_{DE} was lower than the reference value, the crack depth to be detected by the NDI increased, and the safety and rationality of maintenance were further improved.

4.2.5 For components that also require fatigue crack evaluation

In the case of the primary system of a light water reactor, fatigue analysis is not necessary because most of the members have high rigidity. However, fatigue analysis is required for ECCS pipes in the furnace affected by turbulence, instrumentation pipes for temperature, etc. For such members, harmless crack dimensions for stress corrosion cracking and fatigue crack should be evaluated [6], the smaller of which should be detected by NDI.

5. Conclusions

Numerical analysis was carried out to rationalize maintenance against stress corrosion cracking (SCC) and improve reliability using surface-crack-harmless technology via peening in stainless steel welds. The results obtained were as follows:

1) A harmless SCC condition has been defined such that the SCC does not propagate under σ_{DE} and the tensile welding residual stress owing to compressive residual stress via peening.

2) In all the cases, the harmless SCC condition was determined by the deepest crack point (point *A*). This is because the absolute value of the assumed σ_0 was almost always larger than the absolute value of σ_{DE}.

3) In this analysis, a_{hml} ranged over 0.5 to 1.5 mm, and the value could be evaluated from $K_{sc(l)}$ of nearly long cracks.

4) As σ_{DE} decreased, a_{hml} also increased.

5) The magnitude of a_{hml} was in the order of the residual stresses, RS3 < RS2 < RS1. In other words, the larger σ_0, σ_m, and d_0 were, the larger a_{hml}. Furthermore, the larger the $K_{sc(l)}$, the larger was the a_{hml}.

6) In this analysis, a_{hml} did not strictly depend on *As* and was almost constant. However, a_{hml} was the smallest when *As* = 1.0, and largest when *As* = 0.1.

7) It may be inferred from this study that if the crack detected after an NDI is not peened after the welding repair, it is necessary to perform NDI(1), which has an extremely high probability of crack detection.

8) In the case of improving the residual stress distribution via peening (i.e., RS1 and RS2) after welding repair of the cracks detected after the NDI, the minimum a_{hml} would be considerably large. For safety reasons, it is imperative that all the cracks at a depth of 80 % of a_{hml} be detected and peened after welding repair. As a result, the reliability of NDI can be improved and the welding repair portion can be reduced, along with sufficient reliability.

9) In the case of improving the residual stress distribution via peening (RS3) after welding repair of cracks detected after the NDI, the minimum a_{hml} was approximately 0.4 mm, which was nearly equal to the crack detection sensitivity of NDI(2). Therefore, even if a crack cannot be detected, reliability can be ensured.

10) If peening is not performed after the welding repair, it is necessary to detect even extremely shallow cracks and perform welding repair to ensure safety.

Acknowledgements

The authors gratefully acknowledge of Ph.D. Kunio Hasegawa of (former) Hitachi, Ltd., and Prof. K. Takahashi of Yokohama National University for his valuable comments.

Nomenclature

a : Crack depth of semielliptical crack in finite plate
a_{hml} : Maximum harmless SCC crack depth
$a_{NDI(1)}$: Minimum detectable crack depth with a = 0.3 mm via nondestructive inspection
$a_{NDI(2)}$: Minimum detectable crack depth with a = 0.25 mm via nondestructive inspection
$2c$: Crack length of the semielliptical crack
$G_0 - G_4$: Shape correction coefficients of the K^{Pr}
$2l$: Through crack length in an infinite plate
l_e : Equivalent half-crack length
S : Area of the semielliptical crack
$S_{NDI(1)}$: Area of a semielliptical crack with $2c$ = 0.6 mm and a = 0.3 mm
$S_{NDI(2)}$: Area of a semielliptical crack with $2c$ = 1.4 mm and a = 0.25 mm
d_0 : Crossing point
t : Plate thickness
$2w$: Plate width
x : Distance in the depth direction from the surface
As : Aspect ratio
NDI : Nondestructive inspection
SCC : Stress corrosion cracking
$\sigma_1 - \sigma_4$: Coefficients obtained from the fourth-order polynomial
σ_0 : Compression residual stress at surface
σ_m : Maximum compression residual stress
σ_{DE} : Design tensile stress
σ_u : Tensile strength
σ_y : Yield stress
K_{app} : Stress intensity factor due to design tensile stress (σ_{DE})
K^{Pr} : Stress intensity factor due to compressive residual stress
K^{Pr}_{app} : Sum of K_{app} and K^{Pr}
K_{sc} : Threshold SCC stress intensity factor for small cracks
$K_{sc(l)}$: Threshold SCC stress intensity factor for large cracks
α_A : Shape correction factor at the deepest crack part (point *A*)
α_C : Shape correction factor at the surface crack part (point *C*)

References

[1] H. Koten and O. Kamaci, Time-dependent corrosion resistance investigation of hydrophobic magnesium alloys, *Advances in Material Science and Engineering* (2023) 281-292.
[2] S. Kuiling, Z. Zheng, J. Wenchun, L. Yun, S. Houde and Z. Yufu, Generation of compressive residual stress at the root of

tube-to-tubesheet welded joints in a heat exchanger, *International Journal of Pressure Vessels and Piping* (2022) 104848.
[3] BPVC.CC.NC.XI-2023, *Nuclear Components-Section XI: Rules for Inservice Inspection of Nuclear Power Plant Components*, ASME (2023).
[4] W. John, *Flaw Assessment in Pressure Equipment and Welded Structures*, Wiley & Sons (2000).
[5] K. Ando, K. W. Nam, M. H. Kim and K. Takahashi, *Improvement of Safety and Reliability against Stress Corrosion Cracking of Stainless Steel Welds by Application of Surface Crack Harmless Technology*, High Pressure Institute of Japan, 60 (2022) 132-141.
[6] K. Ando, M. H. Kim and K. W. Nam, Analysis on peculiar fracture behaviour of shot peened metal using new threshold stress intensity factor range equation, *Fatigue Fract. Eng. Mater Struct.*, 44 (2021) 306-316.
[7] K. W. Nam, K. Ando, M. H. Kim and K. Takahashi, Improving reliability of high strength material designed against fatigue limit using surface crack nondamaging technology fatigue shot peening, *Fatigue & Fracture of Engineering Materials & Structures*, 44 (2021) 1602-1610.
[8] R. Fueki, Fatigue limit improvement and rendering a surface defect harmless by peening for welded joint, *Ph.D. Thesis*, Yokohama National University (2019).
[9] I. Milne, R. A. Ainsworth, A. R. Dowling and A. T. Stewart, Assessment of the integrity of structures containing defects, *Int. J. PVP*, 32 (1988) 3-104.
[10] K. Ando, R. Fueki, K. W. Nam, K. Matsui and K. Takahashi, A study on the unification of the threshold stress intensity factor for micro crack growth, *Transactions of Japan Society of Spring Engineers*, 64 (2019) 39-44.
[11] J. C. Newman Jr. and I. S. Raju, An empirical stress-intensity factor equation for the surface crack, *Eng. Fract Mech.*, 15 (1981) 185-192.
[12] American Petroleum Institute, *Fitness-for-Service*, 1st Ed., American Petroleum Institute (2000).
[13] W. D. Rummel, P. H. Todd Jr, S. A. Frecska and R. A. Rathke, *The Detection of Fatigue Cracks by Nondestructive Testing Methods*, NASA Contractor Report, NASA-CR-2369, NASA (1974).
[14] Y. Mizutani, Nondestructive inspection of metal fatigue, *Industrial Materials (Japan)*, 56 (2008) 86-89.
[15] M. Ochiai, T. Miura and S. Yamamoto, Lase-ultrasonic nondestructive testing and its application to nuclear industry, *Toshiba Review (Japan)*, 61 (2006) 44-47.
[16] K. Ando, K. W. Nam, M. H. Kim and K. Takahashi, Improvement of reliability of fatigue properties of high strength steel applying surface crack non-damaging technology, *Journal of High Pressure Institute of Japan*, 58 (2020) 263-271.

Kyung-Hee Gu is a graduate student of Marine Design Convergence Engineering at Pukyong National University, Busan, Korea. She is interested in the fatigue life and the harmless crack of structural material.

Ki-Woo Nam (Ph.D.) is working on Department of Materials Science and Engineering, Pukyong National University, Busan, Korea. His research fields are the crack healing and the harmless crack of structural component.

Kotoji Ando (Ph.D.) is Emeritus Prof. of Yokohama National University in Japan. His research fields are increase fatigue limit, making surface crack harmless, and developing structural ceramics with self-crack-healing ability.